The Journal of Infectious Diseases

MAJOR ARTICLE

Correlation Between Early Plasma Interleukin 37 Responses With Low Inflammatory Cytokine Levels and Benign Clinical Outcomes in Severe Acute Respiratory Syndrome Coronavirus 2 Infection

Ang Li,[1,a] Yun Ling,[1,a] Zhigang Song,[1,a] Xiaobo Cheng,[1] Longfei Ding,[1] Rendi Jiang,[2] Weihui Fu,[1] Yan Liu,[1] Huiliang Hu,[1] Songhua Yuan,[1] Jian Chen,[1] Cuisong Zhu,[1] Jun Fan,[1] Jing Wang,[1] Yanling Jin,[1] Miaomiao Zhang,[1] Lingyan Zhu,[1] Peng Sun,[1] Linxia Zhang,[1] Ran Qin,[1] Wei Zhang,[1] Chenli Qiu,[1] Yinzhong Shen,[1] Lin Zhang,[1] Zhengli Shi,[2] Chen Zhao,[1] Tongyu Zhu,[1,b] Hongzhou Lu,[1,b] Xiaoyan Zhang,[1,b] and Jianqing Xu[1,b]

[1]Shanghai Public Health Clinical Center & Institutes of Biomedical Sciences, Fudan University, Shanghai, China, and [2]Key Laboratory of Special Pathogens, Wuhan Institute of Virology, Chinese Academy of Sciences, Wuhan, China

Background. The immune protective mechanisms during severe acute respiratory syndrome coronavirus (SARS-CoV-2) infection remain to be deciphered for the development of an effective intervention approach.

Methods. We examined early responses of interleukin 37 (IL-37), a powerful anti-inflammatory cytokine, in 254 SARS-CoV-2–infected patients before any clinical intervention and determined its correlation with clinical prognosis.

Results. Our results demonstrated that SARS-CoV-2 infection causes elevation of plasma IL-37. Higher early IL-37 responses were correlated with earlier viral RNA negative conversion, chest computed tomographic improvement, and cough relief, consequently resulted in earlier hospital discharge. Further assays showed that higher IL-37 was associated with lower interleukin 6 and interleukin 8 (IL-8) and higher interferon α responses and facilitated biochemical homeostasis. Low IL-37 responses predicted severe clinical prognosis in combination with IL-8 and C-reactive protein. In addition, we observed that IL-37 administration was able to attenuate lung inflammation and alleviate respiratory tissue damage in human angiotensin-converting enzyme 2–transgenic mice infected with SARS-CoV-2.

Conclusions. Overall, we found that IL-37 plays a protective role by antagonizing inflammatory responses while retaining type I interferon, thereby maintaining the functionalities of vital organs. IL-37, IL-8, and C-reactive protein might be formulated as a precise prediction model for screening severe clinical cases and have good value in clinical practice.

Keywords. IL-37; SARS-CoV-2; COVID-19; inflammation; clinical outcomes.

Coronavirus disease 2019 (COVID-19), caused by severe acute respiratory syndrome coronavirus 2 (SARS-CoV-2) infection, poses an unprecedented challenge to global public health, and an effective treatment regimen remains elusive. Although the majority of patients with COVID-19 have a benign clinical course, a fraction of them develop severe clinical complications that may even result in death [1]; early alerting and identification of severe cases is critical and may allow for intensive medical care and prevent death [2, 3].

IL-37 is a recently identified member of the interleukin 1 family. It was originally referred as interleukin 1F7 but renamed as IL-37 after it was shown that it requires an interleukin 18R receptor for its binding and biological activity [4]. As an anti-inflammatory cytokine, IL-37 could be produced by various cells, including human peripheral blood mononuclear cells, macrophages, epithelial cells, and activated B cells [5]; Correspondingly, its receptor expresses on inflammatory cytokine secretory cells such as macrophages, mast cells and basophils [6]. There has been a growing body of evidence that IL-37 plays an important role in a variety of inflammatory diseases [7–9].

In the current study, we first identified a significant correlation between plasma IL-37 levels in patients COVID-19 and their clinical prognosis, with elevated plasma IL-37 likely suppressing inflammatory responses and thereby restraining the occurrence of cytokine storms. The absence of an IL-37 response may predict a severe clinical prognosis in SARS-CoV-2 infection.

METHODS

Study Design

All 254 patients had COVID-19 confirmed by SARS-CoV-2 viral RNA and admitted to the Shanghai Public Health Clinical Center,

Received 28 August 2020; editorial decision 9 November 2020; accepted 12 November 2020; published online November 17, 2020.

[a]A. L., Y. Ling, and Z. Song contributed equally to this article.

[b]J. X., X. Z., H. L. and T. Z. are co-senior authors and contributed equally to this work.

Correspondence: J. Xu, PhD, Shanghai Public Health Clinical Center & Institutes of Biomedical Sciences, Fudan University, Shanghai, China (xujianqing@shphc.org.cn).

The Journal of Infectious Diseases® 2021;223:568–80

DOI: 10.1093/infdis/jiaa713

Shanghai, China, between 6 February 2020 and 27 May 2020. Plasma samples from the 254 patients were collected on admission, before treatment. According to the median level of IL-37, 127 patients with lower IL-37 levels (75 male and 52 female) and 127 (65 male and 62 female) with higher IL-37 levels were enrolled. Table 1 shows the distributions by age, sex, other demographic characteristics, and biochemical and immunologic indexes in the low– and high–IL-37 groups, along with *P* values. All patients were treated according to the *COVID-19 Prevention and Control Plan* [10].

Quantification of Plasma IL-37 and Other Cytokines

Plasma IL-37 from the 254 patients with COVID-19 was assayed using a human IL-37/interleukin 1F7 enzyme-linked immunosorbent assay kit (Beijing 4A; Biotech); 10 cytokines, including interferon (IFN) γ, interleukin 1β, 4, 5, 10, 12P70, and 22, interleukin 6 and 8 (IL-6 and IL-8), and tumor necrosis factor α, were measured using the Simoa CorPlex human cytokine detection kit (catalog no. 85–0329; Quanterix). All biosafety regulations were followed during the assays.

Patient Information Collection

Clinical data for the 254 patients were collected from clinical test reports (routine blood and urine studies, coagulation indexes), biochemical reports (blood gas analysis, liver function, kidney function), immune reports (cytokine determination, absolute cell number determination, complement measurement) computed tomographic (CT) reports, and vital sign monitoring (body temperature, respiration, blood oxygen saturation, blood pressure), among other records (Supplementary Figures 1 and 2).

Animal Experiments

The human angiotensin-converting enzyme 2 (hACE2)–transgenic mice used were 5–6-week-old Institute of Cancer Research female mice, which were purchased from Hua-Fu-Kang and split into 2 groups, with 3 mice in each group. All mice were inoculated intranasally with 50 μL (10^5 median tissue culture infective dose) of SARS-CoV-2 virus (provided by Z. Shi). Mice in the experimental group were then intravenously administered 12.5 μg/kg of recombinant human IL-37 [11] (Novoprotein Technology) at 12 and 48 hours after virus inoculation, and those in the control group were injected with phosphate-buffered saline (PBS). The protocol was approved by Institutional Animal Care and Use Committee at the Wuhan Institute of Virology, China Academy of Sciences, and implemented in an animal biosafety level 3 laboratory. All animal experiments were carried out at the Wuhan Institute of Virology, in

Table 1. Clinical Characteristics and Immunological and Biochemical Indexes in 254 Patients With Coronavirus Disease 2019

Characteristic or Index	All Patients (N = 254)	Low IL-37 Response (n = 127)	High IL-37 Response (n = 127)	*P* Value
Age, mean (SEM), y	42.76 (0.951)	44.88 (1.484)	40.63 (1.167)	.12
Age, median (IQR), y	41 (32–53.25)	42 (32–61)	41 (32–47)	
Sex, no. (%)				
Male	140 (55.12)	75 (53.57)	65 (46.43)	.66
Female	114 (44.88)	52 (45.61)	62 (54.38)	
Underlying disease, no. (%)				
Hypertension	30 (11.81)	20 (15.74)	10 (7.87)	.05
Diabetes	20 (7.87)	10 (7.87)	10 (7.87)	.999
Hepatitis	5 (1.97)	3 (2.36)	2 (1.57)	.65
Pharyngitis	3 (1.18)	2 (1.57)	1 (0.78)	.57
Rhinitis	12 (4.72)	2 (1.57)	10 (7.87)	.02
Asthma	4 (1.57)	3 (2.36)	1 (0.78)	.32
Body temperature, mean (SEM), °C	37.02 (0.037)	37.1 (0.052)	36.94 (0.052)	.02
Body temperature, median (IQR), °C	37 (36.5–37.5)	37.2 (36.5–37.5)	36.8 (36.4–37.5)	
Fever, no. (%)	94 (37)	55 (43.3)	39 (30.7)	
Immunological indexes				
Blood cell counts, $\times 10^9$/L				
Leukocytes, mean (SEM)	5.719 (0.14)	5.546 (0.12)	5.89 (0.23)	.49
Leukocytes, median (IQR)	5.29 (4.34–6.65)	5.23 (4.26–6.34)	5.38 (4.41–6.8)	
Lymphocytes, mean (SEM)	1.51 (0.04)	1.49 (0.06)	1.52 (0.06)	.54
Lymphocytes, median (IQR)	1.4 (1.1–1.83)	1.4 (1.05–1.83)	1.4 (1.14–1.83)	
Monocytes, mean (SEM)	0.47 (0.01)	0.45 (0.02)	0.50 (0.02)	.09
Monocytes, median (IQR)	0.45 (0.35–0.59)	0.42 (0.31–0.58)	0.47 (0.35–0.59)	
Platelets, mean (SEM)	214 (4.52)	205 (6.15)	222 (6.55)	.04
Platelets, median (IQR)	209 (161–256)	201 (155–244)	213 (167–267)	
Basophils, mean (SEM)	0.02 (0.00)	0.02 (0.00)	0.02 (0.00)	.79
Basophils, median (IQR)	0.01 (0.01–0.02)	0.01 (0.01–0.03)	0.01 (0.01–0.02)	

Table 1. Continued

Characteristic or Index	All Patients (N = 254)	Low IL-37 Response (n = 127)	High IL-37 Response (n = 127)	*P* Value
Eosinophils, mean (SEM)	0.05 (0.00)	0.04 (0.01)	0.06 (0.01)	.12
Eosinophils, median (IQR)	0.02 (0.01–0.06)	0.02 (0.00–0.05)	0.03 (0.01–0.07)	
Neutrophils, mean (SEM)	3.70 (0.13)	3.60 (0.15)	3.80 (0.21)	.84
Neutrophils, median (IQR)	3.3 (2.46–4.46)	3.28 (2.48–4.34)	3.46 (2.32–4.56)	
T-cell count, cells/μL				
$CD3^+$, mean (SEM)	1084 (35.9)	1053 (54.75)	1115 (46.42)	.18
$CD3^+$, median (IQR)	963 (729–1352)	963 (640–1334)	962 (762–1388)	
$CD4^+$, mean (SEM)	602 (18.65)	583 (24.89)	622 (27.83)	.51
$CD4^+$, median (IQR)	558 (397–775)	543 (388–775)	571 (412–779)	
$CD8^+$, mean (SEM)	389 (12.5)	352 (17.3)	406 (17.78)	.04
$CD8^+$, median (IQR)	339 (241–500)	308 (212–485)	357 (258–504)	
NK cell count, cells/μL				
$CD16^+CD56^+$, mean (SEM)	230 (9.8)	227 (13.5)	233 (14)	.90
$CD16^+CD56^+$, median (IQR)	209 (147–288)	240 (145–274)	203 (147–309)	
Biochemical indexes				
ALT, mean (SEM), U/L	29.39 (1.53)	29.34 (1.92)	39.44 (2.37)	.40
ALT, median (IQR) (U/L)	21 (14–35)	22 (14–35)	20 (14–31)	
AST, mean (SEM) (U/L)	26.02 (0.95)	27.12 (1.48)	24.95 (1.20)	.38
AST, median (IQR) (U/L)	21 (17–29)	22 (17–30)	20 (17–28)	
LDH, mean (SEM) (U/L)	225 (4.75)	239 (8.06)	212 (4.88)	.049
LDH, median (IQR) (U/L)	204 (181–242)	208 (186–255)	203 (175–233)	
CHE, mean (SEM) (U/L)	9029 (132.8	8839 (174.1)	9216 (199.5)	.27
CHE, median (IQR) (U/L)	8780 (7718–10 146)	8749 (7253–10 002)	8942 (7875–10 269)	
CK, mean (SEM) (U/L)	108.3 (7.17)	120.1 (11.15)	96.4 (8.923)	.01
CK, median (IQR) (U/L)	77 (54–120)	86 (58.5–124)	68 (51–106)	
Myoglobin, mean (SEM) (U/L)	16.38 (1.42)	19.16 (2.14)	13.61 (1.85)	<.001
Myoglobin, median (IQR) (U/L)	10.95 (2.34–22.18)	14.44 (4.51–25.68)	5.27 (1.65–18.28)	
Creatinine, mean (SEM) (μmol/L)	66.61 (1.21)	69.57 (2.12)	63.72 (1.15)	.17
Creatinine, median (IQR) (μmol/L)	64.5 (53.68–74.4)	65.94 (53.67–75.57)	63.42 (53.68–73.4)	
ATPP, mean (SEM) (s)	38.27 (0.47)	38.54 (0.89)	38.01 (0.37)	.59
ATPP, Median (IQR) (s)	37.5 (35–40.2)	37.3 (35.03–40.18)	37.85 (34.98–40.2)	
ESR, mean (SEM) (mm/h)	41.27 (2.18)	46.46 (3.31)	36.33 (2.81)	.03
ESR, median (IQR), mm/h	32 (10–72)	37 (12–76)	28 (10–50)	
Albumin, mean (SEM), g/L	42.82 (0.27)	42.4 (0.40)	43.22 (0.37)	.20
Albumin, median (IQR), g/L	43.19 (40.31–45.71)	42.73 (40.11–45.42)	43.58 (40.63–45.9)	
HDL-C, mean (SEM), mmol/L	1.11 (0.02)	1.09 (0.03)	1.13 (0.03)	.42
HDL-C, median (IQR), mmol/L	1.07 (0.93–1.27)	1.08 (0.91–1.26)	1.07 (0.94–1.29)	
LDL-C, mean (SEM), mmol/L	2.88 (0.06)	2.82 (0.09)	2.94 (0.08)	.28
LDL-C, median (IQR), mmol/L	2.76 (2.28–3.37)	2.81 (2.16–3.39)	2.74 (2.39–3.39)	
D-dimer, mean (SEM), μg/mL	0.58 (0.11)	0.78 (0.22)	0.38 (0.02)	.42
D-dimer, median (IQR), μg/mL	0.32 (0.22–0.47)	0.33 (0.22–0.5)	0.31 (0.23–0.46)	
pH, mean (SEM)	7.39 (0.00)	7.39 (0.00)	7.39 (0.00)	.66
pH, median (IQR)	7.38 (7.36–7.41)	7.38 (7.36–7.41)	7.39 (7.37–7.41)	
Pco_2, mean (SEM), kPa	5.44 (0.04)	5.40 (0.06)	5.49 (0.06)	.49
Pco_2, median (IQR), kPa	5.42 (5.05–5.82)	5.39 (5–5.78)	5.42 (5.10–5.87)	
Po_2, mean (SEM), kPa	13.97 (0.27)	13.86 (0.41)	14.08 (0.34)	.36
Po_2, median (IQR), kPa	13.05 (11.68–15.13)	12.85 (11.33–15.38)	13.3 (11.78–15.13)	
Arterial lactic acid, mean (SEM). mmol/L	2.07 (0.18)	1.98 (0.11)	2.16 (0.35)	.03
Arterial lactic acid, median (IQR), mmol/L	1.5 (1.2–2.15)	1.6 (1.3–2.3)	1.4 (1.1–2)	
Lactate, mean (SEM), mmol/L	2.57 (0.05)	2.65 (0.07)	2.50 (0.07)	.049
Lactate, median (IQR), mmol/L	2.45 (2.02–3)	2.54 (2.20–3.07)	2.29 (2.00–2.89)	

Abbreviations: ALT, alanine aminotransferase; AST, aspartate aminotransferase; ATPP, activated partial thromboplastin time; CHE, cholinesterase; CK, creatine kinase; ESR, erythrocyte sedimentation rate; HDL-C, high-density lipoprotein cholesterol; IL-37, interleukin 37; IQR, interquartile range; LDH, lactic dehydrogenase; LDL-C, low-density lipoprotein cholesterol; NK, natural killer; SEM, standard error of the mean.

strict compliance with the *Guide for the Care and Use of Laboratory Animals,* to ensure the personnel safety and animal welfare.

Histopathological Examination

Mice were euthanized at 5 days after infection, and lung tissues were isolated and fixed with 4% formalin. After sectioning with a microtome, slides were stained by hematoxylin-eosin (HE), following a standard protocol. The scanning procedures were conducted with TissueFAXS Confocal Plus 200 (TissueGnostics), and the images acquired were analyzed using Strata Quest 6.0X software to calculate pathological scores and quantify inflammatory cells.

Statistical Analysis

Student *t* tests were used for parametric continuous data, and unpaired 2-sided Mann-Whitney *U* tests for nonparametric data. Log-rank (Mantel-Cox) tests were used to evaluate significant differences between discharge rates, viral RNA negative conversion rates and cough relief rates in the 2 patient groups. The significant *P* value cutoff was set at .05. A predicted receiver operating characteristic curve of severely classified patients was examined, and the equation was calculated using SPSS 23 software and binary logistic regression analysis. The Python library "numpy-polyfit" was used to fit the smooth receiver operating characteristic curve. Quantitative indexes are reported as mean values (with standard errors of the mean [SEMs]), continuous features as medians (with interquartile ranges), and categorical features as numbers (with percentages).

Ethical Considerations

The cohort study was approved by the Ethics Committee of Shanghai Public Health Clinical Center (no. YJ-2020-S130-01), and all participants enrolled in this study signed informed consent forms. The animal protocol was reviewed and approved by the Institutional Animal Care and Use Committee at Wuhan Institute of Virology, China Academy of Sciences (no. WIVA05202009).

RESULTS

Correlation Between Elevated Plasma IL-37 Responses in Patients With COVID-19 and Benign Clinical Outcome

An enzyme-linked immunosorbent assay was performed to quantify IL-37 levels in 254 patients with COVID-19 at admission (before treatment intervention) and 36 healthy subjects (negative for SARS-CoV-2 RNA). We found that patients with COVID-19 presented significantly higher plasma IL-37 levels (mean [SEM], 196.2 [35.78] pg/mL; 95% confidence interval [CI], 125.7–266.6 pg/mL) than healthy individuals (19.72 [5.60] pg/mL; 8.36–31.09 pg/mL) ($P = .001$) (Figure 1A), suggesting that SARS-CoV-2 infection is likely to result in anti-inflammatory responses, such as those involving IL-37.

We next explored the possible role of increased plasma IL-37 levels. The 254 patients were split into high–IL-37 (n = 127) and low–IL-37 (n = 127) groups, according to the overall median plasma IL-37 value (19.01 pg/mL). Interestingly, the high–IL-37 group experienced significantly shorter hospitalizations than the low–IL-37 group (mean [SEM], 14.8 [0.42] vs 20.3 [0.87] days, respectively; $P < .001$) (Figure 1B); rates of discharge within 9 days were 15.75% (20 of 127) and 1.57% (2 of 127), respectively (Figure 1C). All patients were discharged within 25 days for the high–IL-37 group and within 69 days for the low–IL-37 group ($P < .001$; log-rank test) (Figure 1D).

Correlation of Low Plasma IL-37 Responses With Severe Clinical Prognoses

We further examined the clinical prognoses of patients in the high– and low–IL-37 groups, including the timing and rates of SARS-CoV-2 viral RNA negative conversion, chest CT improvement, and cough relief. As expected, viral RNA negative conversion was significantly later in the low–IL-37 group (mean [SEM], 8.1 [0.6] days; 95% CI, 6.88–9.28 days) than in the high–IL-37 group (4.5 [0.36] days; 3.82–5.26 days) ($P < .001$), with 46% negative viral RNA in the low–IL-37 group versus 74% in the high–IL-37 group within 6 days. In addition, 31 days was required for all 122 patients in the low–IL-37 group to become RNA negative, whereas only 20 days was needed for all 121 patients in the high–IL-37 group ($P < .001$; log-rank test) (Figure 2A).

We next determined chest CT improvement. Chest CT scans of patients with COVID-19 usually showed multiple small patch shadows and interstitial changes at the early stage and then gradually developed into multiple ground-glass opacities or infiltration shadows in both lungs [12, 13]. These lesions become absorbed and dissipate with the improvement of clinical symptoms and disease status [10]. Of 254 patients, 23 exhibited no manifestations at chest CT (10 in the low– and 13 in the high–IL-37 group), 17 had only a single chest CT report (10 in the low– and 7 in the high–IL-37 group), and 18 showed long-term unchanged chest CT observations (9 in the low– and 9 in the high–IL-37 group). After exclusion of those 58 patients, 196 patients remained, 98 patients in each group. Chest CT improvement took more time in the low–IL-37 group (mean [SEM], 9.44 [0.6] days; 95% CI, 8.24–10.64 days) than in the high–IL-37 group (6.43 [0.3] days; 95% CI, 6.15–7.32 days) ($P < .001$; Mann-Whitney *U* test), with 34 of 98 (35%) achieving chest CT improvement within 6 days in the low–IL-37 versus 56 of 98 (57%) in the high–IL-37 group. In addition, it took 27 days to achieve chest CT improvement for all 98 patients in the low–IL-37 group, compared with only 14 days for all 98 patients in the high–IL-37 group ($P < .001$; log-rank test) (Figure 2B).

After SARS-CoV-2 infection, patients often present clinical symptoms of cough [14–16]. Among all 254 patients, 84 presented with cough symptoms, with 37 cases in the low– and 47 in the high–IL-37 group. The low–IL-37 group required more time to achieve cough relief (mean [SEM], 11.67 [3.51]

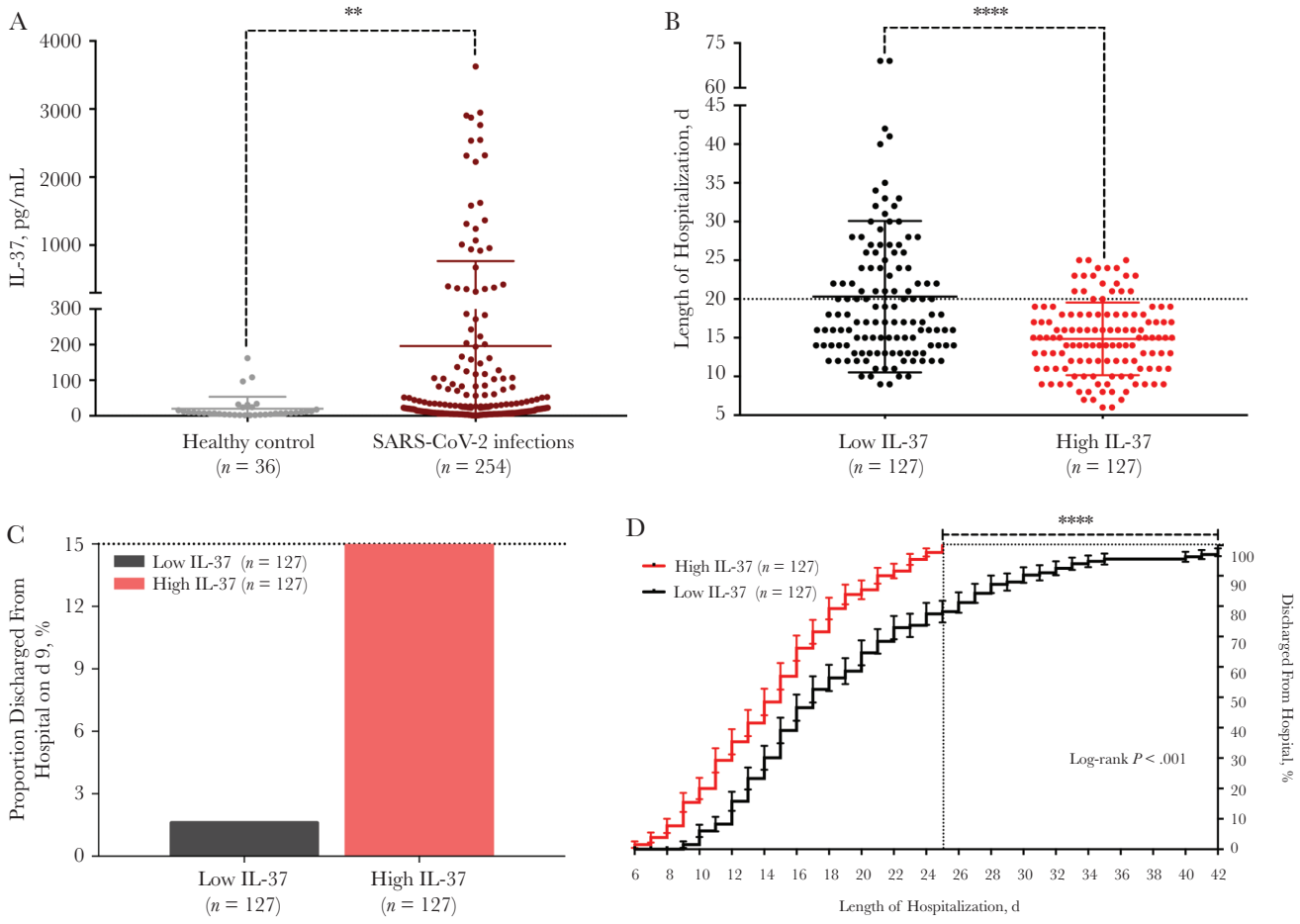

Figure 1. Elevated interleukin 37 (IL-37) levels in patients are correlated with benign clinical outcomes. Plasma IL-37 levels are shown in healthy control individuals (n = 36) and patients with severe acute respiratory syndrome coronavirus 2 (SARS-CoV-2) (n = 254) (**P = .001; unpaired 2-tailed Mann-Whitney U test). *A,* Plot diagram showing the median values (*middle line*), with the first and third quartiles. *B,* Duration of hospitalization for patients in the low–IL-37 (n = 127) and high–IL-37 (n = 127) groups. Dotted line indicates differences on hospital discharged on day 20 between two groups (****P < .0001). *C,* Two-dimensional distribution histogram of discharge rates within 9 days. *D,* Log-rank (Mantel-Cox) tests were used to identify significant differences in discharge rates (****P < .0001); dotted line indicates days after discharge rate reached 100%.

days; 95% CI, 2.647–20.69 days) than the high–IL-37 group (8.72 [0.91] days; 6.855–10.58 days) (P = .002). Only 11 of 37 patients (29.7%) in the low–IL-37 group achieved relief within 5 days, compared with 29 of 47 (61.7%) in the high–IL-37 group. It took 9 days for half of the patients in the low–IL-37 group to achieve relief, compared with only 4 days in the high–IL-37 group (Figure 2C). Overall, these observations suggest that the absence of IL-37 responses in patients with COVID-19 is correlated with severe clinical prognoses, and IL-37 is likely to play a protective role during SARS-CoV-2 infection.

Effect of Low Plasma IL-37 Responses on the Capacity to Maintain Biochemical Homeostasis

We further determined the correlation of IL-37 and various biochemical indicators in the laboratory. We analyzed concentrations of lactate, lactate dehydrogenase, and arterial lactic acid in the groups with low and high IL-37 levels and observed that those metabolic indicators were not maintained in the normal range in many patients in both groups, suggesting the occurrence of hypoxemia and respiratory distress symptoms after SARS-CoV-2 infection. Overall, all 3 indicators were significantly higher in the low– than in the high–IL-37 group (P = .02 for arterial lactic acid; P = .049 for lactate and lactate dehydrogenase (Figure 3A). Thus, patients with low IL-37 responses are likely to have more severe respiratory distress and hypoxemia. Accordingly, the low–IL-37 group exhibited significantly higher myoglobin, creatine kinase, and total bilirubin levels than the high–IL-37 group (P < .001, .01, and .03, respectively), suggesting more damage to heart and liver functions. No significant differences were detected in D-dimer (P = .42), aspartate aminotransferase (P = .40), or alanine aminotransferase (P = .38) levels (Figure 3B and 3C).

In general, infection and inflammation result in an increase in the erythrocyte sedimentation rate, which was significantly higher in the low– than in the high–IL-37 group (P = .03), indicating that IL-37 may help induce inflammatory responses. No significant differences in creatinine or albumin were observed (P = .17 and .20, respectively) (Figure 3D).

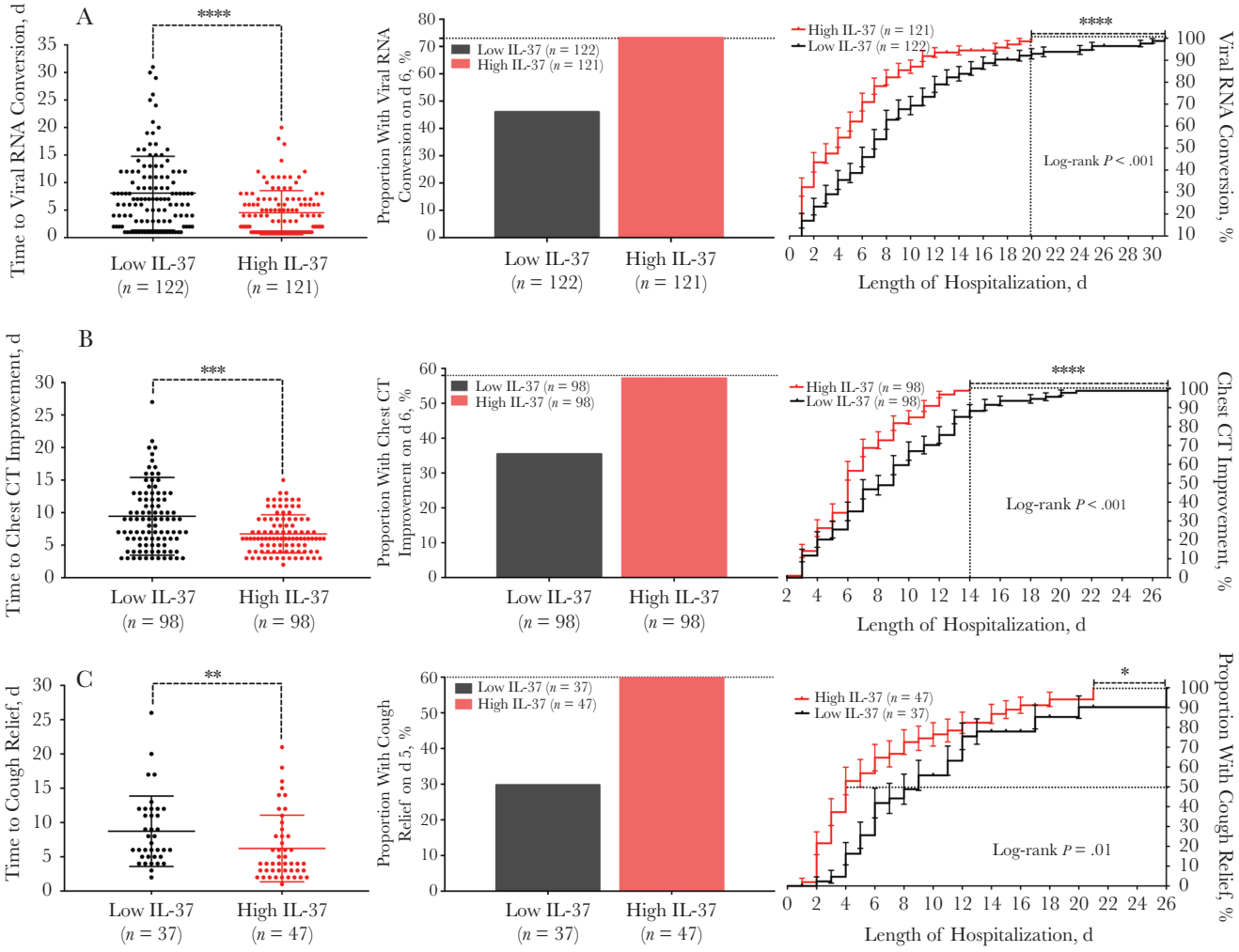

Figure 2. Higher interleukin 37 (IL-37) levels facilitate clinical prognosis in multiple indicators. *A, Left,* Time to viral RNA negative conversion in low–IL-37 (n = 122) and high–IL-37 (n = 121) groups (****$P < .0001$). *Middle,* Two-dimensional distribution histogram of viral RNA negative conversion rate within 6 days. *Right,* Viral RNA negative conversion rates were evaluated using log-rank (Mantel-Cox) tests (****$P < .0001$). *B, Left,* Time to chest computed tomographic (CT) improvement in the 2 groups (***$P < .001$). *Middle,* Two-dimensional distribution histogram of chest CT image improvement rates within 6 days; dotted line corresponds to the y-axis. *Right,* Chest CT improvement rate was evaluated using log-rank (Mantel-Cox) tests (****$P < .0001$). *A* and *B,* dotted lines indicatedays after Viral RNA conversion rate and Chest CT improvement rate reached 100%. *C, Left,* Time to cough relief (**$P = .003$). *Middle,* Two-dimensional distribution histogram of cough relief rates within 5 days. *Right,* Log-rank (Mantel-Cox) tests were conducted to analyze differences in cough relief rates (*$P = .01$). The dotted line indicates days after cough relief rate reached 50%.

Other biochemical indicators, such as Pco_2, Po_2, and blood pH, are shown in Supplementary Figure 1. Overall, IL-37 responses may facilitate the retention of organ functions by antagonizing inflammation and thereby maintaining biochemical homeostasis.

Effect of Low Plasma IL-37 Responses on Innate Immune Balance Maintenance

We also assessed a panel of cytokines in the initial plasma at patient admission, including IL-6, IL-8, and IFN-α. Surprisingly, an imbalance of innate immune responses was noted with significantly higher IL-6 and IL-8 levels and lower IFN-α levels in the low– than in the high–IL-37 group ($P < .001$ for both IL-6 and IL-8; $P = .02$ for IFN-α). IL-6 and IL-8 are inflammatory cytokines and prone to causing immune pathogenesis, whereas IFN-α exerts inhibitory activities against viral replication. Thus, the imbalanced innate responses in the low–IL-37 group conferred a tendency of failure to restrain SARS-CoV-2 replication. Accordingly, high-sensitivity C-reactive protein (HS-CRP) was also significantly higher in the low– than in the high–IL-37 group ($P = .049$) (Figure 4A).

We next examined immune cell numbers in peripheral blood at patient admission. Both myeloid and lymphoid-derived cells generally were in normal ranges, with abnormal levels in only a few patients, indicating that the majority of patients were at an early phase of the disease. Regardless, the low–IL-37 group presented significantly lower $CD8^+$ T-cell and platelet counts than the high–IL-37 group ($P = .04$ for $CD8^+$ T cells and .04 for

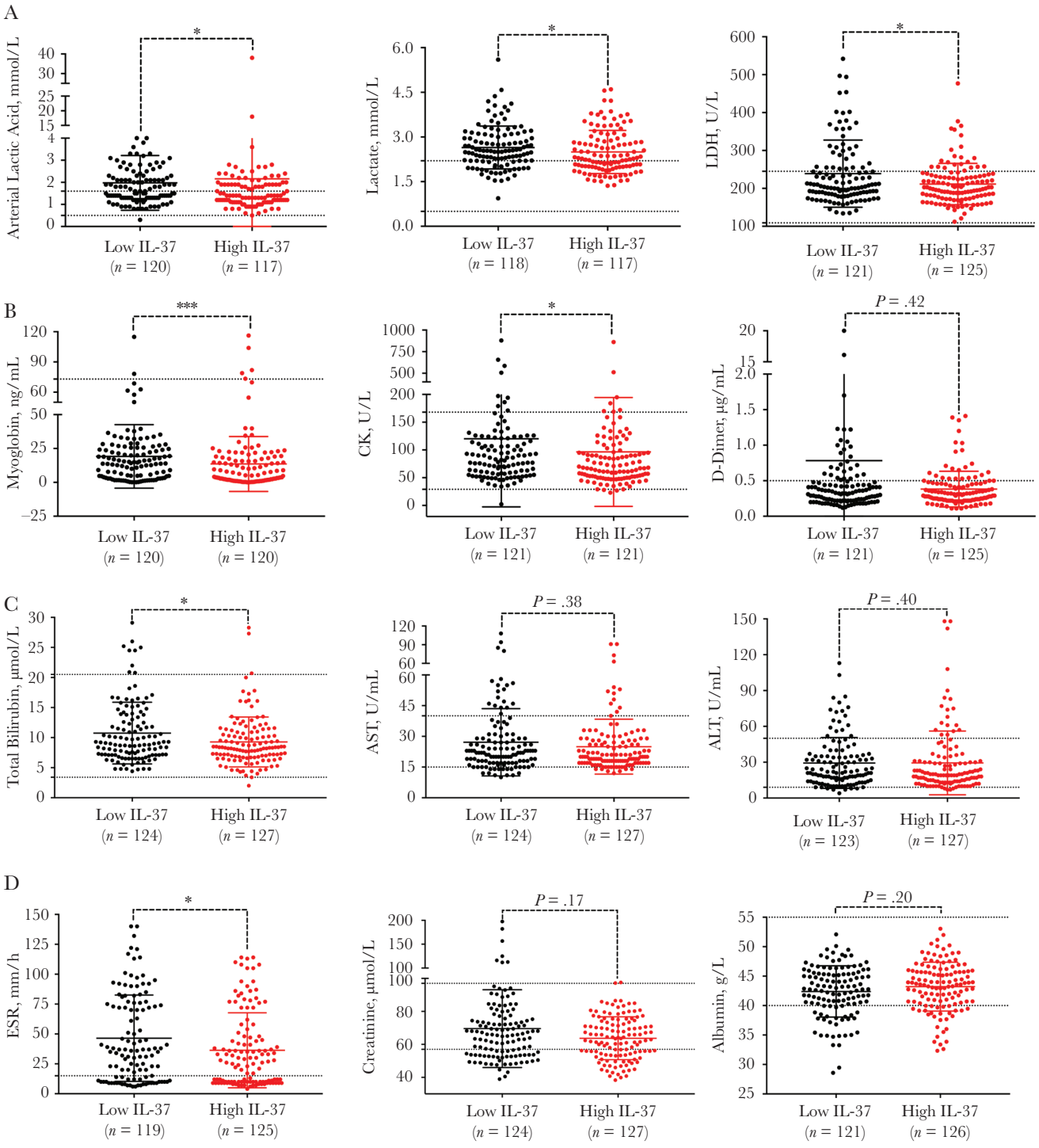

Figure 3. Statistical analysis between interleukin 37 (IL-37) secretion levels and biochemical indicators. *A,* Differences in arterial lactic acid, lactate, and lactate dehydrogenase (LDH) levels between the low– and high–IL-37 groups. *B,* Myoglobin, creatine kinase (CK), and D-dimer levels in the 2 groups. *C,* Statistical analyses of total bilirubin, aspartate aminotransferase (AST), and alanine aminotransferase (ALT) levels. *D,* A significant difference in erythrocyte sedimentation rate (ESR) was detected between the 2 groups. Creatinine and albumin levels were also analyzed. Dotted lines represent normal ranges of indicators. Data were analyzed using unpaired 2-tailed Mann-Whitney *U* tests. *P* values are represented as **P* < .05,**P < .01, ****P* < .001,*****P* < .0001.

platelets, respectively), whereas no significant differences were observed for all other cells, including white blood cells (total cells of both myeloid and lymphoid-derived cells), monocytes, lymph cells, natural killer cells, and $CD3^+$ and $CD4^+$ T cells (Figure 4B and C). Other immunological indicators are shown in Supplementary Figure 2.

Overall, a low IL-37 response seems to attenuate host capacity to suppress inflammation and results in elevated inflammatory

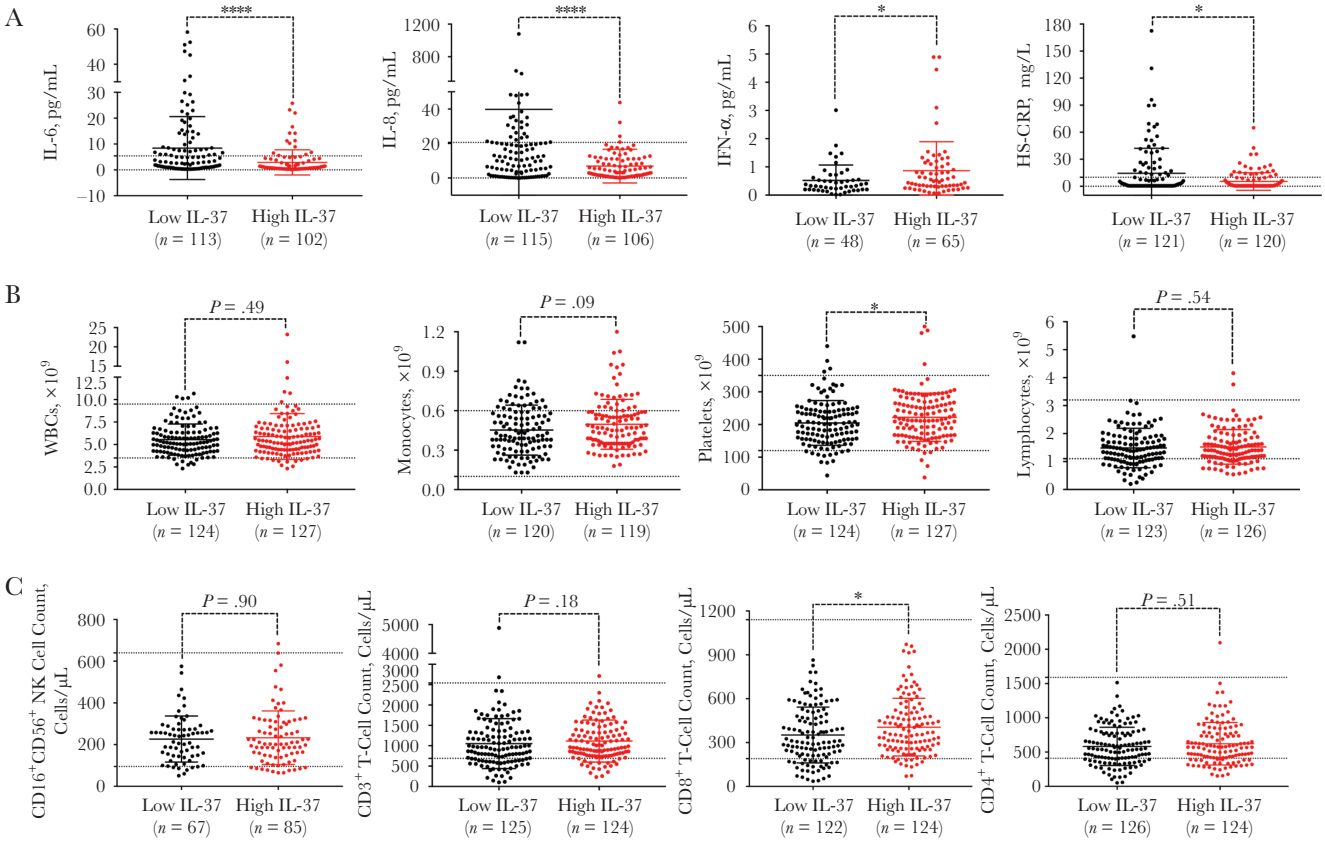

Figure 4. Correlation analysis between interleukin 37 (IL-37) secretion level and immunological detection indexes. *A,* Significant differences in interleukin 6 (IL-6; $P < .0001$), interleukin 8 (IL-8; $P < .0001$), and interferon (IFN) α (0.0171) levels between the low– and high–IL-37 groups. Differences in high-sensitivity C-reactive protein (HS-CRP) levels were less marked ($P = .049$) *B,* Differences in leukocyte, monocyte, platelet, and lymphocyte counts. *C,* Statistical analysis of the absolute numbers of $CD16^+CD56^+$ natural killer (NK) and $CD3^+$, $CD8^+$, and $CD4^+$ T cells. Data were analyzed using unpaired 2-tailed Mann-Whitney *U* tests. Dotted lines represent normal ranges of indicators. *P* values are represented as $^*P < .05$, $^{**}P < .01$, $^{***}P < .001$, $^{****}P < .0001$.

cytokine levels. Importantly, elevated IFN-α levels was noted in the high–IL-37 group, suggesting that IL-37 is unlikely to interfere with IFN responses.

Combination of Low IL-37 Levels and Inflammatory Indicators in Predicting Severe COVID-19

Among the 254 cases, 20 were clinically sorted into the severe category. Interestingly, all 20 severe cases presented very low initial plasma IL-37 and elevated HS-CRP and IL-8 levels on admission before any treatment (Figure 5A). Furthermore, significant reverse correlations were identified between IL-37 and both HS-CRP ($P = .04$) and IL-8 ($P = .01$) (Figure 5B). The sensitivity of IL-37 alone to differentiate severe from moderate cases was 100%, with an area under the curve (AUC) of 0.747 and a specificity of 55.7%. To improve the prediction value, we added HS-CRP to IL-37 and observed that the AUC increased to 0.933 and that the specificity reached 91.2%, but the sensitivity decreased to 92.9% (Figure 5C and Supplementary Table 1). Because the omission of severe cases might result in loss of life, we further explored a more sensitive model by incorporating IL-8. Importantly, the sensitivity of the combination of IL-37, HS-CRP, and IL-8 reached 100%, with an AUC of 0.959 (95% CI, .932–.986) and a specificity of 91.2%. The final regression equation for this joint prediction model was as follows:

$$\text{Logit}(P) = -2.77 - 0.0072 \cdot \text{IL-37 (pg/mL)} + 0.009 \cdot \text{IL-8 (pg/mL)} + 0.048 \cdot \text{HS-CRP (mg/L)},$$
$$P = e^{\text{Logit}(P)}/[1 + e^{\text{logit}(P)}].$$

Because IL-6 has been implicated to be involved in disease pathogenesis caused by SARS-CoV-2 infection, we examined its relationship with disease prognosis and with IL-37. As expected, plasma IL-6 levels in the group with severe disease were significantly higher than in the moderate-disease group (Supplementary Figure 3*A*), IL-6 levels were inversely correlated with serum IL-37 levels, and high IL-37 levels were accompanied by low IL-6 levels (Supplementary Figure 3*B*). We also assessed the predictive value of IL-6, alone or in combination with IL-37 or both IL-37 and HS-CRP, for clinical outcomes of SARS-CoV-2 infection. As shown in Supplementary Figure 3C, the algorithm of a triple combination of IL-6, IL-37, and HS-CRP was most predictive, followed by IL-6 plus IL-37 and then IL-6 alone. However, the predictive power of combined

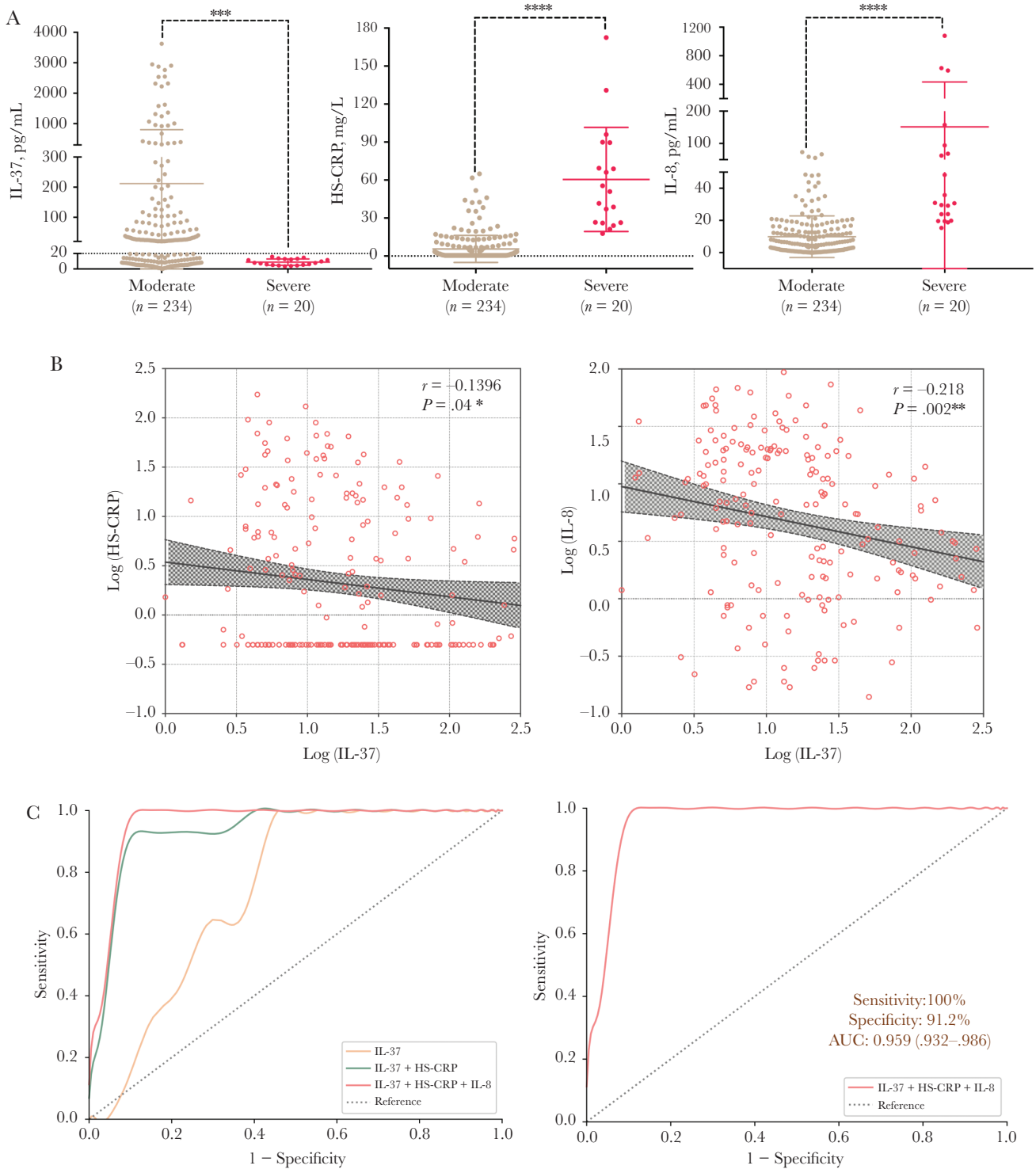

Figure 5. Prediction value of interleukin 37 (IL-37) in severe classification of coronavirus disease 2019. *A,* Significant differences in IL-37, high-sensitivity C-reactive protein (HS-CRP) and interleukin 8 (IL-8) levels between moderate and severe infections. *B,* Significant reverse correlations between IL-37 and HS-CRP and between IL-37 and IL-8. *C, Left,* Receiver operating characteristic (ROC) curves for different combinations: IL-37 alone; IL-37 and HS-CRP; and IL-37, HS-CRP, and IL-8. *Right,* ROC curve for IL-37, HS-CRP, and IL-8, along with sensitivity, specificity, and area under the curve (AUC; with 95% confidence interval). The smooth ROC curves above were fitted by the Python library "numpy-polyfit." Dotted lines represent a curve when the occurrence of an event is completely random, the farther the prediction curve deviates from the reference line, the stronger the prediction ability is. *P* values are represented as **P* < .05,***P* < .01, ****P* < .001,*****P* < .0001.

IL-6, IL-37, and HS-CRP was still much less than that of combined IL-8, IL-37, and HS-CRP (Figure 5C) Taking these findings together, we identified the triple-marker of IL-8, IL-37, and HS-CRP as remarkably predictive of the clinical severity of diseases caused by SARS-CoV-2. Because all 3 evaluations can be performed on patient admission, before treatment, this prediction model may have great value in clinical practice for patients with COVID-19.

IL-37 and Pulmonary Inflammation in hACE2 -Transgenic Mice Infected With SARS-CoV-2

To further validate the anti-inflammatory ability of IL-37 during SARS-CoV-2 infection, we used a transgenic mice model that expressed hACE2 and was infected with SARS-CoV-2. After infection, the mice were split into 2 groups. The first group received intravenous IL-37 (dissolved in PBS) at 2 time points, 12 and 48 hours after infection, and the other (control) group was administered PBS only. As expected, lung tissue histopathological examination revealed more severe inflammatory cell infiltration and tissue injuries in control group, with more interstitial thickening and edema, blood capillary congestion and hemorrhage, and exfoliation of pulmonary alveoli epithelium on day 5 after infection than in the experimental group (Figure 6A and 6B). To quantify the lung damage overall, we adopted a pathological score and inflammatory cell quantification algorithm. The control group was scored significantly higher than the IL-37 treatment group (P = .006) (Figure 6C), accordingly, more inflammatory cells per unit tissue area were found in the control group (P = .02) (Figure 6D).

DISCUSSION

The COVID-19 pandemic due to SARS-CoV-2 infection has caused mass mortality worldwide and has become the most severe public health challenge; moreover, effective treatment for patients with COVID-19 remains unavailable. Because hypercytokinemia and respiratory inflammation are known as critical pathogenesis mechanisms during respiratory viral infection [17–19] and IL-37 is a power suppressor against inflammation, we rationalized that IL-37 may play a protective role during SARS-CoV-2 infection and should therefore be explored for treatment. Here, we report that among 254 patients with COVID-19, early IL-37 responses before any treatment correlate with clinical outcomes. Elevated IL-37 responses probably favor balancing innate responses and thus efficiently restrain viral replication to maintain the functionalities of host vital organs and thereby maintain internal homeostasis. In contrast, failure to mount IL-37 responses is likely to indicate a severe clinical prognosis.

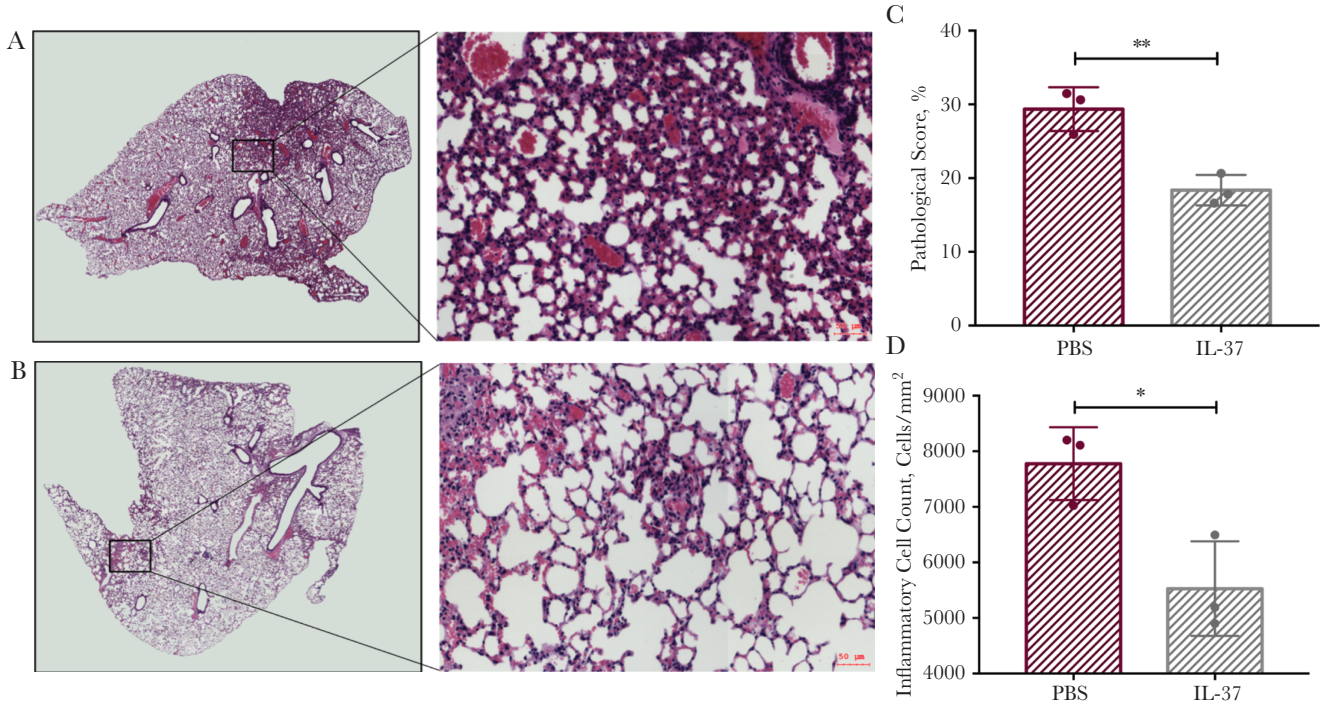

Figure 6. Interleukin 37 (IL-37) alleviates inflammation in human angiotensin-converting enzyme 2–transgenic mice infected with severe acute respiratory syndrome coronavirus 2. *A, B,* Representative hematoxylin-eosin (HE)–stained sections on day 5 after infection (scale bars represent 1 mm [*left*] and 50 μm [*right*]). *A,* HE-stained lung sections from control group treated with phosphate-buffered saline (PBS) (n = 3), with increased hemorrhage and inflammatory cell influx. *B,* HE-stained lung sections from experimental group treated with IL-37 (n = 3), with milder tissue injuries. *C,* Pathological scores were calculated on the basis of lung histochemical data (P = .006). *D,* Inflammatory cells were quantified in each lung tissue section (P = .02). Quantification data were analyzed as means with standard deviations, using unpaired *t* tests; the P value cutoff was .05. P values are represented as $^{*}P < .05$, $^{**}P < .01$, $^{***}P < .001$, $^{****}P < .0001$.

Several studies have confirmed that the high inflammatory responses resulting from SARS-CoV-2 infection, presented as cytokine release syndrome [20], are among the preliminary pathogeneses for disease and death in patients with COVID-19 [21–23]. In severe COVID-19 cases, dynamic IL-6 and IL-8 levels are associated with disease progression [24]. Similarly, we identified elevation in IL-6 and IL-8 levels and their association with clinical pathogenesis. To antagonize inflammatory responses, corticosteroids are usually administered clinically; however, their efficacy in COVID-19–induced cytokine release syndrome is controversial, because it may increase viral replication and stimulate additional inflammatory responses. An ideal intervention is to retain intact innate immune responses but restrain inflammatory responses, and a novel treatment strategy with fine-tuning of the immune system is urgently needed [25].

IL-37 is a newly discovered cytokine with strong anti-inflammatory activities. To date, researchers have focused more on its protective role and application in autoimmune diseases. Studies showed that increased plasma IL-37 correlates significantly with ameliorated clinical manifestations in systemic lupus erythematosus [26], rheumatoid arthritis [27] and inflammatory bowel disease [28].

The unique anti-inflammatory mechanism may confer IL-37 with a wide range of anti-inflammatory activities. Early researchers found that IL-37 can enter the nucleus and form a functional complex with Smad3 [9], thereby reducing anti-inflammatory function by regulating gene transcription [29]. In recent years, a new anti-inflammatory mechanism involving binding to interleukin 18Ra was discovered. IL-37 is able to inhibit downstream proinflammatory signal kinases, such as mammalian target of rapamycin (mTOR) and mitogen-activated protein kinase (MAPK). IL-37 also activates the anti-inflammatory signaling molecules Mer and PTEN [7, 30, 31].

The detailed mechanism of IL-37 against respiratory diseases has also been explored. Huang et al [32] found that IL-37 may reduce airway inflammation by suppressing activation of NF-κB and signal transducer and activator of transcription 1 type 3 in asthma. Kim et al [33] identified that IL-37 can inhibit transforming growth factor β 1–induced lung fibroblast proliferation, promoting the progression of idiopathic pulmonary fibrosis disease. Qi et al [11] observed that IL-37 attenuates secretion of inflammatory cytokines by down-regulating the MAPK signal transduction pathway in an H1N1 infection model, protecting mice from lung damage and improving survival. Zhou et al [34] found that IL-37 induced by H3N2 infection can directly restrain the replication of influenza virus.

In the current study, we demonstrated that IL-37 is likely to play a protective role during SARS-CoV-2 infection. Early elevated plasma IL-37 before treatment correlates with low inflammatory cytokines, high IFN-α, a high number of immune cells, and reduced hypoxemia. Furthermore, we demonstrated that IL-37 can effectively antagonize inflammatory responses in hACE2-transgenic mice after SARS-CoV-2 infection, the early administration of IL-37 reduced inflammatory cell infiltration and alleviated lung tissue damage, thereby facilitating disease remission. Recently, Hadjadj et al [35] found that exacerbated inflammatory responses and impaired type I IFN activity are hallmarks of severe illness, implicating the protective role of type I IFN. An important observation in our study is that the level of IFN-α in patients with high plasma IL-37 levels was significantly higher than in the low–IL-37 group, suggesting that IL-37 is unlikely to suppress and even might enhance production of IFN-α. These findings highlight the potential of IL-37 in the development of a novel therapeutic regimen, not only against coronaviruses such as SARS-CoV-2 and MERS, but also against influenza and other respiratory viruses.

It is crucial to identify severe cases early before development of clinical complications and thus gain time to prevent severe illness and death. We used IL-37 alone or in combination with other factors to formulate an effective prediction model. With incorporation of IL-37, IL-8, and HS-CRP, sensitivity reached 100%, and specificity reached 91.2%. Because all data for this model were collected from samples obtained at patient admission and before any clinical intervention, the prediction may be applicable at the moment of admission, and we believe the model is likely to prove valuable in the future, after validation in a large-scale longitudinal cohort.

Supplementary Data

Supplementary materials are available at The Journal of Infectious Diseases online. Consisting of data provided by the authors to benefit the reader, the posted materials are not copyedited and are the sole responsibility of the authors, so questions or comments should be addressed to the corresponding author.

Notes

Acknowledgments. We acknowledge all patients involved in the study and all the medical staff who provided clinical test data.

Author contributions. J. X. configured the project, and X. Z. and J. X. designed the project and supervised the experiments. T. Z. and H. L. coordinated the study. A. L. performed the experiments, analyzed the data, and drafted the manuscript. Z. Song implemented the viral RNA assay. R. J. performed animal experiments. C. Z. scanned the lung tissue sections. All authors collected the blood samples and clinical data. J. X. revised the manuscript. X. Z. and J. X. acquired the funding.

Financial support. This work was supported by the National Science Foundation of China (grants 81771704 and 81761128007]; the National 13th Five-Year Grand Program on Key Infectious Disease Control (grant 2018ZX10301403-003), and the Shanghai Science and Technology Committee (grant 18DZ2293000).

Potential conflicts of interest. A. L., X. Z., and J. X. have 2 pending patents: "A quantifiable, interleukin-37-based respiratory virus infection early warning model for severe (critical) cases" and "Application of interleukin 37 and interferon in the treatment of viral infections." All other authors report no potential conflicts. All authors have submitted the ICMJE Form for Disclosure of Potential Conflicts of Interest. Conflicts that the editors consider relevant to the content of the manuscript have been disclosed.

References

1. Tang D, Comish P, Kang R. The hallmarks of COVID-19 disease. PLoS Pathog **2020**; 16:e1008536.
2. Subbarao K, Mahanty S. Respiratory virus infections: understanding COVID-19. Immunity **2020**; 52:905–9.
3. Liang W, Yao J, Chen A, et al. Early triage of critically ill COVID-19 patients using deep learning. Nat Commun **2020**; 11:3543.
4. Nold MF, Nold-Petry CA, Zepp JA, Palmer BE, Bufler P, Dinarello CA. IL-37 is a fundamental inhibitor of innate immunity. Nat Immunol **2010**; 11:1014–22.
5. Chen Z, Wang S, Li L, Huang Z, Ma K. Anti-inflammatory effect of IL-37-producing T-cell population in DSS-induced chronic inflammatory bowel disease in mice. Int J Mol Sci **2018**; 19:3884.
6. Gutzmer R, Langer K, Mommert S, Wittmann M, Kapp A, Werfel T. Human dendritic cells express the IL-18R and are chemoattracted to IL-18. J Immunol **2003**; 171:6363–71.
7. Cavalli G, Dinarello CA. Suppression of inflammation and acquired immunity by IL-37. Immunol Rev **2018**; 281:179–90.
8. Xu WD, Zhao Y, Liu Y. Insights into IL-37, the role in autoimmune diseases. Autoimmun Rev **2015**; 14:1170–5.
9. Huang Z, Xie L, Li H, et al. Insight into interleukin-37: the potential therapeutic target in allergic diseases. Cytokine Growth Factor Rev **2019**; 49:32–41.
10. National Health Commission of the People's Republic of China. COVID-19 prevention and control plan. 4th ed. National Health Commission of the People's Republic of China, **2020**.
11. Qi F, Liu M, Li F, et al. Interleukin-37 ameliorates influenza pneumonia by attenuating macrophage cytokine production in a MAPK-dependent manner. Front Microbiol **2019**; 10:2482.
12. Zhu N, Zhang D, Wang W, et al. A novel coronavirus from patients with pneumonia in China, 2019. N Engl J Med **2020**; 382:727–33.
13. National Health Commission of the People's Republic of China. COVID-19 treatment guidelines. 5th ed. National Health Commission of the People's Republic of China, **2020**.
14. Guan WJ, Ni ZY, Hu Y, et al. Clinical characteristics of coronavirus disease 2019 in China. N Engl J Med **2020**; 382:1708–20.
15. Chen N, Zhou M, Dong X, et al. Epidemiological and clinical characteristics of 99 cases of 2019 novel coronavirus pneumonia in Wuhan, China: a descriptive study. Lancet **2020**; 395:507–13.
16. Wang D, Hu B, Hu C, et al. Clinical characteristics of 138 hospitalized patients with 2019 novel coronavirus-infected pneumonia in Wuhan, China. JAMA **2020**; 323:1061–9.
17. Wong JP, Viswanathan S, Wang M, Sun LQ, Clark GC, D'Elia RV. Current and future developments in the treatment of virus-induced hypercytokinemia. Future Med Chem **2017**; 9:169–78.
18. Pelaia C, Tinello C, Vatrella A, De Sarro G, Pelaia G. Lung under attack by COVID-19-induced cytokine storm: pathogenic mechanisms and therapeutic implications. Ther Adv Respir Dis **2020**; 14:1753466620933508.
19. Wang Z, Zhang A, Wan Y, et al. Early hypercytokinemia is associated with interferon-induced transmembrane protein-3 dysfunction and predictive of fatal H7N9 infection. Proc Natl Acad Sci U S A **2014**; 111:769–74.
20. Coperchini F, Chiovato L, Croce L, Magri F, Rotondi M. The cytokine storm in COVID-19: An overview of the involvement of the chemokine/chemokine-receptor system. Cytokine Growth Factor Rev **2020**; 53:25–32.
21. Merad M, Martin JC. Pathological inflammation in patients with COVID-19: a key role for monocytes and macrophages. Nat Rev Immunol **2020**; 20:355–62.
22. Song JW, Zhang C, Fan X, et al. Immunological and inflammatory profiles in mild and severe cases of COVID-19. Nat Commun **2020**; 11:3410.
23. Azkur AK, Akdis M, Azkur D, et al. Immune response to SARS-CoV-2 and mechanisms of immunopathological changes in COVID-19. Allergy **2020**; 75:1564–81.
24. Li S, Jiang L, Li X, et al. Clinical and pathological investigation of patients with severe COVID-19. JCI Insight **2020**; 5:138070.
25. Liu B, Li M, Zhou Z, Guan X, Xiang Y. Can we use interleukin-6 (IL-6) blockade for coronavirus disease 2019 (COVID-19)-induced cytokine release syndrome (CRS)? J Autoimmun **2020**; 111:102452.
26. Ye L, Ji L, Wen Z, et al. IL-37 inhibits the production of inflammatory cytokines in peripheral blood mononuclear cells of patients with systemic lupus erythematosus: its correlation with disease activity. J Transl Med **2014**; 12:69.
27. Wang L, Wang Y, Xia L, Shen H, Lu J. Elevated frequency of IL-37- and IL-18Rα-positive T cells in the peripheral blood of rheumatoid arthritis patients. Cytokine **2018**; 110:291–7.
28. Fonseca-Camarillo G, Furuzawa-Carballeda J, Yamamoto-Furusho JK. Interleukin 35 (IL-35) and IL-37: intestinal and peripheral expression by T and B regulatory cells in patients with inflammatory bowel disease. Cytokine **2015**; 75:389–402.

29. Grimsby S, Jaensson H, Dubrovska A, Lomnytska M, Hellman U, Souchelnytskyi S. Proteomics-based identification of proteins interacting with Smad3: SREBP-2 forms a complex with Smad3 and inhibits its transcriptional activity. FEBS Lett **2004**; 577:93–100.
30. Nold-Petry CA, Lo CY, Rudloff I, et al. IL-37 requires the receptors IL-18Rα and IL-1R8 (SIGIRR) to carry out its multifaceted anti-inflammatory program upon innate signal transduction. Nat Immunol **2015**; 16:354–65.
31. Li S, Neff CP, Barber K, et al. Extracellular forms of IL-37 inhibit innate inflammation in vitro and in vivo but require the IL-1 family decoy receptor IL-1R8. Proc Natl Acad Sci U S A **2015**; 112:2497–502.
32. Huang N, Liu K, Liu J, et al. Interleukin-37 alleviates airway inflammation and remodeling in asthma via inhibiting the activation of NF-κB and STAT3 signalings. Int Immunopharmacol **2018**; 55:198–204.
33. Kim MS, Baek AR, Lee JH, et al. IL-37 attenuates lung fibrosis by inducing autophagy and regulating TGF-β1 production in mice. J Immunol **2019**; 203:2265–75.
34. Zhou F, Zhu CL, Niu ZL, Xu FX, Song H, Liu XH. Influenza A virus inhibits influenza virus replication by inducing IL-37. J Clin Lab Anal **2019**; 33:e22638.
35. Hadjadj J, Yatim N, Barnabei L, et al. Impaired type I interferon activity and inflammatory responses in severe COVID-19 patients. Science **2020**; 369:718–24.